

# Matter-wave amplification and phase conjugation via stimulated dissociation of a molecular Bose-Einstein condensate

Karén V. Kheruntsyan

*ARC Centre of Excellence for Quantum-Atom Optics, Department of Physics, University of Queensland,  
Brisbane, Queensland 4072, Australia*

(Received 10 January 2005; published 18 May 2005)

We propose a scheme for parametric amplification and phase conjugation of an atomic Bose-Einstein condensate (BEC) via stimulated dissociation of a BEC of molecular dimers consisting of bosonic atoms. This can potentially be realized via coherent Raman transitions or using a magnetic Feshbach resonance. We show that the interaction of a small incoming atomic BEC with a (stationary) molecular BEC can produce two counter-propagating atomic beams - an amplified atomic BEC and its phase-conjugate or “time-reversed” replica. The two beams can possess strong quantum correlation in the relative particle number, with squeezed number-difference fluctuations.

DOI: 10.1103/PhysRevA.71.053609

PACS number(s): 03.75.Kk, 03.65.Yz, 42.50.-p

The fascinating experimental progress in controlling ultracold atomic gases has now resulted in the creation of quantum-degenerate samples of ultracold molecules and molecular Bose-Einstein condensates (BEC). The first step toward seeing molecular condensation was undertaken in transient experiments with a BEC of  $^{85}\text{Rb}$  atoms [1], in which interference measurements were indicative of a small molecular condensate formation. More recent experiments with  $^{133}\text{Cs}$ ,  $^{87}\text{Rb}$ , and  $^{23}\text{Na}$  [2], as well as with degenerate Fermi gases of  $^{40}\text{K}$  and  $^6\text{Li}$  atoms [3], have produced even larger samples of ultracold molecules, including molecular condensates.

All these experiments have employed conversion of atom pairs into weakly bound molecular dimers in the vicinity of a magnetically tunable Feshbach resonance. This technique appears to be more successful at present than Raman photoassociation [4,5]. Unambiguous claims on the observation of equilibrium molecular condensates have only been made for the case of molecules consisting of fermionic atoms. These molecules have much longer lifetimes because of Pauli blocking, which suppresses their decay due to inelastic collisions [6]. Despite this, the production of Bose condensed dimers composed of bosonic atoms should not be out of reach using current experimental techniques.

The purely bosonic case is particularly interesting since the underlying dynamics in the atom-molecule conversion can take advantage of coherence and bosonic stimulation with respect to both the atomic and molecular species. In practical terms, this could lead to a wider range of techniques for coherent quantum control of ultracold quantum gases, including the possibility of superchemistry [5], matter-wave amplification with atom-molecular “laser” beams, as well as various implementations of nonlinear atom optics and quantum atom optics.

Here, we propose a scheme for nonlinear, coherent matter-wave amplification and phase conjugation, which at the same time is capable of producing pair-correlated or number-squeezed atomic beams. The scheme relies on the process of stimulated dissociation of a BEC of molecular dimers, taking place in the presence of an injected signal—a

small incoming atomic condensate. The resulting output consists of an amplified signal and its “time-reversed” or phase-conjugate replica [7].

This is analogous to the nonlinear optical process of parametric amplification of a “seed” signal, using frequency conversion of photons in a quadratically nonlinear media [8]. In the matter-wave parametric amplification, the coupling that takes the role of the “quadratic nonlinearity” and converts molecules into atom pairs and vice versa can be realized via coherent Raman transitions or using magnetic Feshbach resonances. Either of these mechanisms have certain advantages and disadvantages from the practical point of view, however, the essential physics can be modeled via an effective quantum-field theory, which is identical in the two cases [9–11].

The advantage of the present scheme compared to spontaneous molecule dissociation [12–16], with no atomic condensate present initially, is that the desired quantum effects with mesoscopic atom numbers can be achieved on much shorter time scales. As a result, the disruptive effect of inelastic collisions on molecule lifetimes can be bypassed, thus making the present scheme much more robust for practical implementation. In addition, the scheme has an advantage compared to earlier related proposals [17] using four-wave mixing [18] in that it is less susceptible to phase noise in the “pump” BEC—once its depletion is taken into account.

We start by considering the Heisenberg equations of motion for the coupled atomic-molecular system in a one-dimensional (1D) environment, which in a rotating frame and in a dimensionless form, are given by [9,13]

$$\frac{\partial \hat{\psi}_1}{\partial \tau} = i \frac{\partial^2 \hat{\psi}_1}{\partial \xi^2} - i \delta \hat{\psi}_1 + \kappa \hat{\psi}_2 \hat{\psi}_1^\dagger,$$

$$\frac{\partial \hat{\psi}_2}{\partial \tau} = \frac{i}{2} \frac{\partial^2 \hat{\psi}_2}{\partial \xi^2} - i [V_2(\xi) + u_{22} \hat{\psi}_2^\dagger \hat{\psi}_2] \hat{\psi}_2 - \frac{1}{2} \kappa \hat{\psi}_1^2. \quad (1)$$

Here,  $\hat{\psi}_1(\xi, \tau) = \sqrt{d_0} \hat{\Psi}_1(x, t)$  and  $\hat{\psi}_2(\xi, \tau) = \sqrt{d_0} \hat{\Psi}_2(x, t)$  represent the dimensionless atomic and molecular field operators

(such that  $\langle \hat{\Psi}_i^\dagger \hat{\Psi}_i \rangle$  gives the 1D linear density), with bosonic commutation relations  $[\hat{\psi}_i(\xi, \tau), \hat{\psi}_j^\dagger(\xi', \tau)] = \delta_{ij} \delta(\xi - \xi')$ , where  $\xi = x/d_0$  is the dimensionless coordinate,  $\tau = t/t_0$  is the dimensionless time,  $d_0$  is a length scale, and  $t_0 = 2m_1 d_0^2/\hbar$  is a time scale. In addition,  $m_1$  and  $m_2 = 2m_1$  are the atomic and molecular masses,  $\delta = \Delta t_0$  is the dimensionless detuning (with  $2\hbar\Delta$  giving the overall energy mismatch between a pair of free atoms and a molecule),  $\kappa = \chi t_0/\sqrt{d_0}$  is the dimensionless atom-molecule coupling (with  $\chi$  being the respective 1D coupling), and  $u_{22} = U_{22} t_0/d_0$  is the dimensionless coupling for molecule-molecule  $s$ -wave-scattering interaction (with  $U_{22}$  being the respective 1D coupling [19,20]). Finally,  $V_2(\xi) = -u_{22} n_2^0 (1 - \xi^2/\xi_0^2)$  describes the axial trapping potential for the molecules, which we assume is harmonic, where  $n_2^0 = \langle \hat{\psi}_2^\dagger(0,0) \hat{\psi}_2(0,0) \rangle$  is the dimensionless initial peak density of the molecular condensate and  $\xi_0$  is the respective Thomas-Fermi radius.

We assume a highly elongated cigar-shaped trap geometry such that the system can be modeled by a 1D theory [19,20], as above. The atoms are assumed to be untrapped axially, while confined transversely. The molecules are trapped both transversely and axially.

In the case of Raman photodissociation, the energy mismatch is given by  $2\hbar\Delta = 2E_1 - E_2 - \hbar\omega$ , where  $\omega$  is the frequency difference between the two Raman lasers, while  $2E_1$  and  $E_2$  refer, respectively, to the energy of free-atom pairs in the dissociation limit and the energy of the bound molecular state.

In the case of a Feshbach resonance [15,16],  $2\hbar\Delta$  gives the energy mismatch achieved upon switching on the atom-molecule coupling, i.e., upon a rapid crossing of the magnetic field through the resonance, which “brings” the (initially stable) molecular level above the atomic dissociation limit. This corresponds to having  $\Delta < 0$ , and results in dissociation of molecules into atom pairs such that the potential energy  $2\hbar|\Delta|$  is converted into the atomic kinetic energy  $[2\hbar|\Delta| \approx 2\hbar^2 k^2/(2m_1)]$  for selected phase-matched modes with opposite momenta around  $\pm k_0 = \sqrt{2m_1|\Delta|/\hbar}$ . This strategy of a fast ramp through the resonance is very similar to the one realized experimentally in Ref. [16], where a quasi-mono-energetic spherical wave of atoms was created. A realization of this experiment in a one-dimensional environment would correspond to the conditions of the current proposal.

In our model, the interaction terms due to atom-atom and atom-molecule  $s$ -wave-scattering processes are neglected on the grounds that we only consider large absolute values of the detuning  $|\Delta|$  and restrict ourselves to short dissociation times. As a result, the number of atoms produced during dissociation remains small, and the mean-field or phase diffusion terms due to atom-atom and atom-molecule scatterings remain negligible compared to  $|\Delta|$ .

Before analyzing the quantum dynamics of the system described by Eqs. (1), we first consider a simplified model that has an analytic solution. This corresponds to an undepleted, uniform molecular condensate in a coherent state at density  $n_2^0$ , in which case the molecular field amplitude (which we assume is real) can be absorbed into an effective coupling  $g = \kappa\sqrt{n_2^0}$ . Expanding  $\hat{\psi}_1(\xi, \tau)$  in terms of single-

mode annihilation operators,  $\hat{\psi}_1(\xi, \tau) = \sum_q \hat{a}_q(\tau) e^{iq\xi}/\sqrt{l}$ , where  $q = kd_0$  is the dimensionless momentum,  $l$  is the quantization length, and the operators  $\hat{a}_q$  satisfy the usual commutation relations  $[\hat{a}_q(\tau), \hat{a}_{q'}^\dagger(\tau)] = \delta_{q,q'}$ , we obtain the following Heisenberg equations of motion:

$$\begin{aligned} d\hat{a}_q/d\tau &= -i[q^2 + \delta]\hat{a}_q + g\hat{a}_{-q}^\dagger, \\ d\hat{a}_{-q}^\dagger/d\tau &= i[q^2 + \delta]\hat{a}_{-q}^\dagger + g\hat{a}_q. \end{aligned} \quad (2)$$

These have the following well-known solution [13,21]:  $\hat{a}_q(\tau) = A_q(\tau)\hat{a}_q(0) + B_q(\tau)\hat{a}_{-q}^\dagger(0)$  and  $\hat{a}_{-q}^\dagger(\tau) = B_q(\tau)\hat{a}_q(0) + A_q^*(\tau)\hat{a}_{-q}^\dagger(0)$ , where

$$\begin{aligned} A_q(\tau) &= \cosh(g_q\tau) - i\lambda_q \sinh(g_q\tau)/g_q, \\ B_q(\tau) &= g \sinh(g_q\tau)/g_q, \end{aligned} \quad (3)$$

and  $|A_q|^2 - B_q^2 = 1$ . Here, the parameter  $\lambda_q \equiv q^2 + \delta$  can be identified with an *effective* phase mismatch, while  $g_q \equiv (g^2 - \lambda_q^2)^{1/2}$  is the gain coefficient, which—if real—causes a growing output in mode  $q$ , while—if imaginary—leads to oscillations.

To study parametric amplification in the atomic field, we consider initial conditions where all momentum components with  $q > 0$  are initially in a coherent state  $\hat{a}_q(0)|\alpha_q\rangle = \alpha_q|\alpha_q\rangle$ , where  $\alpha_q$  are the corresponding amplitudes, while all negative momentum components are initially in the vacuum state  $\hat{a}_{-q}(0)|0\rangle = 0$ .

Next, we introduce particle number operators  $\hat{N}_+ = \sum_{q>0} \hat{a}_q^\dagger \hat{a}_q$  and  $\hat{N}_- = \sum_{q>0} \hat{a}_{-q}^\dagger \hat{a}_{-q}$  corresponding to the total number of atoms with positive and negative momenta, respectively, and find that the respective average numbers are given by

$$\langle \hat{N}_+(\tau) \rangle = \sum_{q>0} [B_q^2(\tau)(1 + |\alpha_q|^2) + |\alpha_q|^2], \quad (4)$$

$$\langle \hat{N}_-(\tau) \rangle = \sum_{q>0} B_q^2(\tau)(1 + |\alpha_q|^2). \quad (5)$$

For  $\delta < 0$ , the function  $B_q^2$  has two distinct global maxima at  $\pm q_0 = \sqrt{|\delta|}$  corresponding to a zero-effective-phase mismatch,  $\lambda_q = 0$ . In the expression for  $\langle \hat{N}_+(\tau) \rangle$ , the three terms under the sum are identified as the amplified contribution of the vacuum noise in the mode  $q$ ,  $B_q^2(\tau)$ , the amplified coherent component of the input,  $B_q^2(\tau)|\alpha_q|^2$ , and the coherent input component itself,  $|\alpha_q|^2$ , while  $\langle \hat{N}_-(\tau) \rangle$  consists of the amplified vacuum noise and the phase conjugate of the input.

To quantify the correlation and relative number squeezing between  $\hat{N}_+$  and  $\hat{N}_-$ , we consider the normalized variance  $V(\tau)$  of the particle number difference  $\hat{N}_+(\tau) - \hat{N}_-(\tau)$ . In normally ordered form,  $V(\tau)$  is given by

$$V(\tau) = 1 + \langle :[\Delta(\hat{N}_+ - \hat{N}_-)]^2: \rangle / (\langle \hat{N}_+ \rangle + \langle \hat{N}_- \rangle). \quad (6)$$

Here,  $\Delta \hat{X} \equiv \hat{X} - \langle \hat{X} \rangle$ , and  $V(\tau) < 1$  implies squeezing of fluctuations below the coherent level, which is due to strong

quantum correlation between the particle numbers in  $\hat{N}_+(\tau)$  and  $\hat{N}_-(\tau)$ .

Calculating the quantities  $\langle:(\hat{N}_{+,-})^2:\rangle$  and  $\langle\hat{N}_+\hat{N}_-\rangle$  in Eq. (6) and assuming that  $|\alpha_q|^2 \gg 1$  gives the following approximate result for the variance:

$$V(\tau) \approx 1 - \frac{2 \sum_{q>0} B_q^2(\tau) |\alpha_q|^2}{\sum_{q>0} [2B_q^2(\tau) + 1] |\alpha_q|^2}. \quad (7)$$

As we see, the degree of squeezing depends on the magnitude of the amplification factor  $B_q^2(\tau)$ , and for strong amplification,  $B_q^2(\tau) \gg 1$ , one can obtain almost perfect (100%) squeezing,  $V(\tau) \approx 0$ .

We now turn to the exact quantum dynamical simulation of the *nonuniform* system, Eqs. (1). Here, we take into account molecular field depletion, molecule-molecule *s*-wave scattering, and we include possible (linear) losses of atoms and molecules, occurring at rates  $\gamma_1$  and  $\gamma_2$ , respectively. The simulation is done via numerical solution of the stochastic (*c*-number) differential equations [13] in the positive-*P* representation [22]

$$\begin{aligned} \frac{\partial \psi_1}{\partial \tau} &= i \frac{\partial^2 \psi_1}{\partial \xi^2} - (\gamma_1 + i\delta) \psi_1 + \kappa \psi_2 \psi_1^\dagger + \sqrt{\kappa} \psi_2 \eta_1, \\ \frac{\partial \psi_2}{\partial \tau} &= \frac{i}{2} \frac{\partial^2 \psi_2}{\partial \xi^2} - [\gamma_2 + iV_2(\xi) + iu_{22} \psi_2^\dagger \psi_2] \psi_2 - \frac{\kappa}{2} \psi_1^2 \\ &\quad + \sqrt{-iu_{22}} \psi_2 \eta_2, \end{aligned} \quad (8)$$

together with the equations for the “conjugate” fields  $\psi_{1,2}^\dagger$ , having noise terms  $\eta_{1,2}^\dagger$ . Apart from the new loss terms, these equations are equivalent to Eqs. (1), where  $\psi_i$  and  $\psi_i^\dagger$  are independent complex stochastic fields corresponding, respectively, to the operators  $\hat{\psi}_i$  and  $\hat{\psi}_i^\dagger$ , while  $\eta_i$  and  $\eta_i^\dagger$  ( $i=1,2$ ) are four real independent  $\delta$ -correlated Gaussian noises with  $\langle \eta_i(\xi, \tau) \eta_j(\xi', \tau') \rangle = \langle \eta_i^\dagger(\xi, \tau) \eta_j^\dagger(\xi', \tau') \rangle = \delta_{ij} \delta(\xi - \xi') \delta(\tau - \tau')$ .

Figure 1 represents an example of a quantum dynamical simulation of Eqs. (8) illustrating parametric amplification and phase-conjugation of an incident atomic BEC with a center-of-mass momentum  $q_0 = \sqrt{|\delta|}$ . Here, the top frame corresponds to the initial condition of a stable molecular condensate (shown in the middle) in a coherent state with a Thomas-Fermi density profile. The small incoming atomic BEC (shown on the left and moving to the right) is also assumed to be in a coherent state initially, and since we neglect the atom-atom interactions in this low-density regime, we assume a Gaussian density profile. The dissociation coupling  $\kappa$  is invoked at time  $\tau_1$  when the atomic cloud is aligned with the molecular BEC (frame 5 from top). It is kept switched on for a short duration  $\Delta\tau$  such that the amplified and the “reflected” output beams have densities comparable to that of the input beam and can be seen on the same graph.

The next set of simulations is carried out for a more realistic set of parameter values than in Fig. 1. We use a longer dissociation time and a larger coupling  $\kappa$  to result in a large

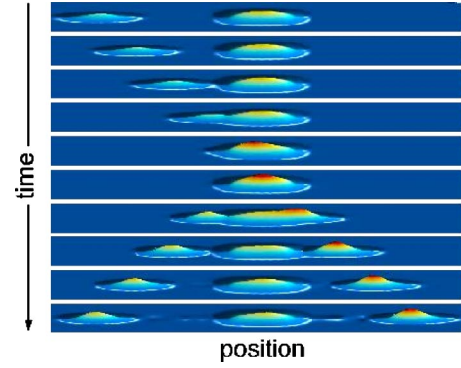


FIG. 1. Atomic and molecular (shown in the middle) density profiles, illustrating parametric amplification and phase conjugation of an incoming atomic BEC (top frame, left) via stimulated molecule dissociation [23]. The results are obtained using 5000 stochastic trajectory averages for  $\kappa=84$ ,  $u_{22}=1.8$ ,  $\delta=-4.9 \times 10^4$ ,  $\gamma_1=0.5$ , and  $\gamma_2=0$ . The dissociation coupling is switched on at  $\tau_1=0.01$  for a duration of  $\Delta\tau=4 \times 10^{-4}$ , while the total time window is  $\tau_f=0.0204$ .

amplification factor and hence a strongly correlated output with squeezing in the particle number difference. For simplicity, the simulation starts from  $\tau=\tau_1=0$  when the incoming atomic cloud is already aligned with the molecular condensate and we invoke the atom-molecule coupling  $\kappa$ . The dissociation is then stopped ( $\kappa=0$ ) at  $\tau=\tau_2$ , and we continue the dynamical evolution of the atomic field in free space (in 1D) to allow spatial separation of the modes with positive and negative momenta during the time interval from  $\tau_2$  to  $\tau_f$ .

For spatially separated components, we can introduce a pair of particle number operators

$$\hat{N}_{+(-)}(\tau) = \int_{0(-l/2)}^{l/2(0)} \hat{\psi}_1^\dagger(\xi, \tau) \hat{\psi}_1(\xi, \tau) d\xi. \quad (9)$$

Next, we define the normalized variance  $V(\tau)$  of the particle number difference as in Eq. (6) and numerically evaluate the relevant averages, using the standard correspondence between the normally ordered operator moments and the *c*-number stochastic averages [22].

Figure 2 shows the results for the atomic density distribution  $n_1(\xi, \tau_f) = \langle \hat{\psi}_1^\dagger(\xi, \tau_f) \hat{\psi}_1(\xi, \tau_f) \rangle$  at final time  $\tau=\tau_f$  and the variance  $V(\tau)$  as a function of  $\tau$ . In this simulation, the initial

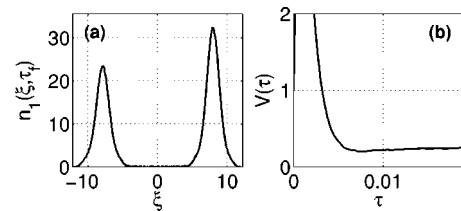


FIG. 2. (a) Final atomic density profile  $n_1(\xi, \tau_f)$  and (b) the variance  $V(\tau)$  as a function of time  $\tau$ . Here, the simulation (with 40 000 stochastic trajectory averages) starts at  $\tau_1$ , the duration of dissociation is  $\Delta\tau=8 \times 10^{-4}$ , and  $\tau_f=1.9 \times 10^{-2}$ . Other parameter values are  $\kappa=297$ ,  $u_{22}=0.068$ ,  $\delta=-5.5225 \times 10^4$ ,  $\gamma_1=\gamma_2=3$ ,  $n_2^0=89.3$ , and  $\xi_0=3.49$  [24].

total number of molecules is 415, the initial number of atoms in the incoming BEC is 21, whereas the final average number of atoms in the two output beams is  $\sim 60$  and 78. The squeezing in the particle number difference at  $\tau = \tau_f$  is about 75% [ $V(\tau_f) \approx 0.25$ ], and it is achieved on a time scale of  $\Delta\tau = \tau_2 - \tau_1 = 8 \times 10^{-4}$  corresponding to 12.7 ms, with the parameter values used here [24]. This is much shorter than the time scale required in spontaneous dissociation [13] to reach the same total number of atoms. At the same time, the degree of squeezing is still rather high.

Thus, the disruptive effect of molecule losses due to inelastic collisions can be reduced in the present scheme. The reason for the shorter time scales required here is that the process of dissociation in the presence of a “seed” atomic BEC begins in the stimulated regime, with exponentially growing output. In the case of spontaneous dissociation, on the other hand, the initial dynamics is in the spontaneous regime and the system spends a relatively long time here before the bosonic stimulation into the phase-matched modes becomes dominant.

To summarize, we have analyzed the process of stimulated dissociation of a condensate of molecular dimers in the presence of a small incoming atomic BEC. This results in parametric amplification of the input BEC together with generation of its phase-conjugate replica, propagating in the opposite direction. The two output beams are strongly correlated in the particle number and have squeezed number-difference fluctuations. The squeezing with a mesoscopic total number of atoms can be achieved on much shorter time scales than in the case of spontaneous dissociation. This makes the present scheme more feasible for practical implementation, using short-lived molecular condensates. In addition, the scheme provides a range of opportunities for coherent quantum control of ultracold quantum gases, including applications of nonlinear and quantum atom optics.

The author thanks P. D. Drummond and M. Olsen for helpful discussions, and the authors of the XmdS software [25] used for simulations. This work was supported by the Australian Research Council and by the National Science Foundation under Grant No. PHY99-07949.

- 
- [1] E. A. Donley *et al.*, *Nature (London)* **417**, 529 (2002).  
 [2] J. Herbig *et al.*, *Science* **301**, 1510 (2003); S. Dürr *et al.*, *Phys. Rev. Lett.* **92**, 020406 (2004); K. Xu *et al.*, *ibid.* **91**, 210402 (2003).  
 [3] C. A. Regal *et al.*, *Nature (London)* **424**, 47 (2003); M. Greiner *et al.*, *ibid.* **426**, 537 (2003); J. Cubizolles *et al.*, *Phys. Rev. Lett.* **91**, 240401 (2003); K. E. Strecker *et al.*, *ibid.* **91**, 080406 (2003); M. Zwierlein *et al.*, *ibid.* **91**, 250401 (2003).  
 [4] R. H. Wynar *et al.*, *Science* **287**, 1016 (2000).  
 [5] D. J. Heinzen *et al.*, *Phys. Rev. Lett.* **84**, 5029 (2000).  
 [6] D. S. Petrov *et al.*, *Phys. Rev. Lett.* **93**, 090404 (2004).  
 [7] An earlier proposal for matter-wave phase conjugation using four-wave mixing in a multicomponent BEC has been discussed by E. V. Goldstein and P. Meystre, *Phys. Rev. A* **59**, 1509 (1999).  
 [8] A. Yariv, *Optical Electronics*, 3rd ed. (Holt Rinehart and Winston, New York, 1985).  
 [9] P. D. Drummond, K. V. Kheruntsyan, and H. He, *Phys. Rev. Lett.* **81**, 3055 (1998).  
 [10] J. Javanainen and M. Mackie, *Phys. Rev. A* **59**, R3186 (1999).  
 [11] E. Timmermans *et al.*, *Phys. Rep.* **315**, 199 (1999).  
 [12] U. V. Poulsen and K. Mølmer, *Phys. Rev. A* **63**, 023604 (2001).  
 [13] K. V. Kheruntsyan and P. D. Drummond, *Phys. Rev. A* **66**, 031602(R) (2002).  
 [14] V. A. Yurovsky and A. Ben-Reuven, *Phys. Rev. A* **67**, 043611 (2003).  
 [15] T. Mukaiyama *et al.*, *Phys. Rev. Lett.* **92**, 180402 (2004).  
 [16] S. Dürr *et al.*, *Phys. Rev. A* **70**, 031601(R) (2004).  
 [17] H. Pu and P. Meystre, *Phys. Rev. Lett.* **85**, 3987 (2000); L.-M. Duan *et al.*, *ibid.* **85**, 3991 (2000).  
 [18] L. Deng, *Nature (London)* **398**, 218 (1999); J. M. Vogels *et al.*, *Phys. Rev. Lett.* **89**, 020401 (2002); **90**, 030403 (2003).  
 [19] M. Olshanii, *Phys. Rev. Lett.* **81**, 938 (1998).  
 [20] K. V. Kheruntsyan *et al.*, *Phys. Rev. Lett.* **91**, 040403 (2003).  
 [21] B. Yurke *et al.*, *Phys. Rev. A* **35**, 3586 (1987).  
 [22] P. D. Drummond and C. W. Gardiner, *J. Phys. A* **13**, 2353 (1980); M. J. Steel *et al.*, *Phys. Rev. A* **58**, 4824 (1998); P. D. Drummond and J. F. Corney, *ibid.* **60**, R2661 (1999).  
 [23] For illustration purposes, we use different scales for the atomic and molecular densities, so that both clouds can be seen on the same graph. The transverse profiles, which were integrated out to arrive at the 1D model in the first place, are recovered here for a 3D visualization.  
 [24] Assuming a  $^{87}\text{Rb}_2$  experiment, these parameters correspond to the molecular trapping potential with the axial frequency  $\omega_x/2\pi = 0.01$  Hz (giving the harmonic oscillator length  $l_x = \sqrt{\hbar/m_2\omega_x} = 76.5$   $\mu\text{m}$ , which we choose to be our length scale,  $d_0 = l_x$ ), radial frequency  $\omega_\perp/2\pi = 82$  Hz ( $l_\perp = 0.84$   $\mu\text{m}$ ), a 3D value of the atom-molecule coupling  $\chi^{(3D)} = 4.95 \times 10^{-7}$   $\text{m}^{3/2} \text{s}^{-1}$  (so that the 1D coupling is  $\chi = \chi^{(3D)}/\sqrt{4\pi l_\perp^2} = 0.165$   $\text{m}^{1/2} \text{s}^{-1}$ ), and a molecule-molecule 3D scattering length  $a_{22} = 0.318$  nm ( $U_{22} \approx U_{22}^{(3D)}/(2\pi l_\perp^2) = 4\pi\hbar a_{22}/(2\pi m_2 l_\perp^2) = 3.28 \times 10^{-7}$   $\text{m} \text{s}^{-1}$ ). The relatively small value of  $a_{22}$  is chosen here for making the computation feasible; it corresponds to  $a_{22} = 0.06a_{11}$ , where  $a_{11} = 5.3$  nm is the scattering length for  $^{87}\text{Rb}$  atoms.  
 [25] <http://www.xmds.org>